



Since January 2020 Elsevier has created a COVID-19 resource centre with free information in English and Mandarin on the novel coronavirus COVID-19. The COVID-19 resource centre is hosted on Elsevier Connect, the company's public news and information website.

Elsevier hereby grants permission to make all its COVID-19-related research that is available on the COVID-19 resource centre - including this research content - immediately available in PubMed Central and other publicly funded repositories, such as the WHO COVID database with rights for unrestricted research re-use and analyses in any form or by any means with acknowledgement of the original source. These permissions are granted for free by Elsevier for as long as the COVID-19 resource centre remains active.



Lung Opacity and Coronary Artery Calcium Score: A Combined Tool for Risk Stratification and Outcome Prediction in COVID-19 Patients

Vitali Koch, MD[†], Leon D. Gruenewald, MD[†], Moritz H. Albrecht, MD, Katrin Eichler, MD, Tatjana Gruber-Rouh, MD, Ibrahim Yel, MD, Leona S. Alizadeh, MD, Scherwin Mahmoudi, MD, Jan-Erik Scholtz, MD, Simon S. Martin, MD, Lukas Lenga, MD, Thomas J. Vogl, MD, Nour-Eldin A. Nour-Eldin, MD, Florian Bienenfeld, MD, Renate M. Hammerstingl, MD, Christiana Graf, MD, Christof M. Sommer, MD, Stefan E. Hardt, MD, Silvio Mazziotti, MD, Giorgio Ascenti, MD, Giovanni Antonio Versace, MD, Tommaso D'Angelo, MD[‡], Christian Booz, MD[‡]

Purpose: To assess and correlate pulmonary involvement and outcome of SARS-CoV-2 pneumonia with the degree of coronary plaque burden based on the CAC-DRS classification (Coronary Artery Calcium Data and Reporting System).

Methods: This retrospective study included 142 patients with confirmed SARS-CoV-2 pneumonia (58 ± 16 years; 57 women) who underwent non-contrast CT between January 2020 and August 2021 and were followed up for 129 ± 72 days. One experienced blinded radiologist analyzed CT series for the presence and extent of calcified plaque burden according to the visual and quantitative HU-based CAC-DRS Score. Pulmonary involvement was automatically evaluated with a dedicated software prototype by another two experienced radiologists and expressed as Opacity Score.

Results: CAC-DRS Scores derived from visual and quantitative image evaluation correlated well with the Opacity Score ($r=0.81$, 95% CI 0.76-0.86, and $r=0.83$, 95% CI 0.77-0.89, respectively; $p<0.0001$) with higher correlation in severe than in mild stage SARS-CoV-2 pneumonia ($p<0.0001$). Combined, CAC-DRS and Opacity Scores revealed great potential to discriminate fatal outcomes from a mild course of disease (AUC 0.938, 95% CI 0.89-0.97), and the need for intensive care treatment (AUC 0.801, 95% CI 0.77-0.83). Visual and quantitative CAC-DRS Scores provided independent prognostic information on all-cause mortality ($p=0.0016$ and $p<0.0001$, respectively), both in univariate and multivariate analysis.

Conclusions: Coronary plaque burden is strongly correlated to pulmonary involvement, adverse outcome, and death due to respiratory failure in patients with SARS-CoV-2 pneumonia, offering great potential to identify individuals at high risk.

Key Words: Coronary Plaque Burden; CAC-DRS Score; SARS-CoV-2 Pneumonia; Coronary Heart Disease; Computed Tomography.

© 2022 The Association of University Radiologists. Published by Elsevier Inc. This is an open access article under the CC BY license (<http://creativecommons.org/licenses/by/4.0/>)

Abbreviations: CAC Coronary artery calcium, CAC-DRS Coronary Artery Calcium Data and Reporting System, CI Confidence interval, COVID-19 Coronavirus disease 2019, DECT Dual-energy computed tomography, hs-TnT hs-Troponin T, HU Hounsfield Unit, SARS-CoV-2 Severe acute respiratory syndrome coronavirus type 2

Acad Radiol 2022; 29:861–870

From the Division of Experimental Imaging, Department of Diagnostic and Interventional Radiology, University Hospital Frankfurt, Frankfurt am Main, Germany (V.K., L.D.G., M.H.A., I.Y., C.B.); Department of Diagnostic and Interventional Radiology, University Hospital Frankfurt, Frankfurt am Main, Germany (K.E., T.G.-R., L.S.A., S.M., J.-E.S., S.S.M., L.L., T.J.V., F.B., R.M.H.); Department of Internal Medicine, University Hospital Frankfurt, Frankfurt am Main, Germany (C.G.); Department of Diagnostic and Interventional Radiology, University Hospital Heidelberg, Heidelberg, Germany (C.M.S.); Department of Cardiology, Angiology and Pulmonology, Heidelberg University Hospital, Heidelberg, Germany (S.E.H.); Department of Biomedical Sciences and Morphological and Functional Imaging, University Hospital Messina, Messina, Italy (S.M., G.A., T.D.); Department of Clinical and Experimental Medicine, University Hospital Messina, Messina, Italy (G.A.V.); Department of Radiology and Nuclear Medicine, Erasmus MC, Rotterdam, The Netherlands (T.D.); Institute for Diagnostic and Interventional Radiology, Frankfurt University Hospital, Frankfurt, Germany (N.-E.A.N.-E.); Department of Diagnostic and Interventional Radiology, Cairo University Hospital, Cairo, Egypt (N.-E.A.N.-E.). Received February 8, 2022; revised February 21, 2022; accepted February 21, 2022. **Address correspondence to:** T. D.'A. e-mail: tommasodang@gmail.com

[†] Vitali Koch and Leon D. Gruenewald contributed equally to this work. [‡] Tommaso D'Angelo and Christian Booz contributed equally to this work.

© 2022 The Association of University Radiologists. Published by Elsevier Inc. This is an open access article under the CC BY license (<http://creativecommons.org/licenses/by/4.0/>)
<https://doi.org/10.1016/j.acra.2022.02.019>

INTRODUCTION

Since the first case of severe acute respiratory syndrome coronavirus 2 (SARS-CoV-2) in December 2019, the novel coronavirus has spread rapidly across the globe (1). While most infected patients remain asymptomatic or present mild symptoms, SARS-CoV-2 is capable of causing respiratory distress syndrome and multiorgan failure, ultimately requiring ventilation support and intensive care (2).

Previous studies reported an underlying cardiovascular disease in up to 50% of patients with SARS-CoV-2, which was associated with adverse outcome and higher mortality (3–5). However, potential mechanistic pathways responsible for fatal outcomes in patients with cardiovascular history remain incompletely understood (6–8). Therefore, identification of patients at risk represents one of the most important goals to prevent complications arising from a delayed treatment.

Over the past decade, many scoring systems have been developed to facilitate standardized reporting and management of different diseases, offering specific treatment recommendations according to disease severity (9,10). Regarding the evaluation of coronary artery calcium (CAC), the CAC-DRS (Coronary Artery Calcium Data and Reporting System) Score has been established (11). CAC scanning is part of the risk assessment to identify atherosclerotic cardiovascular disease offering a direct evaluation of coronary calcified plaque burden (12). Per 2019 ACC/AHA Guideline on the Primary Prevention of Cardiovascular Disease, CAC testing is recommended for asymptomatic individuals at the age of 40–75 years with intermediate risk for atherosclerotic cardiovascular disease or selectively in patients with borderline risk who show a family history of premature coronary artery disease (12,13). In this context, accumulating evidence points to a pivotal role of CAC for predicting outcomes of SARS-CoV-2 patients with coronary heart disease or heart failure (5,8,14–16). To the best of our knowledge, no previous study has examined the value of CAC-DRS reporting in risk assessment and outcome prediction of patients suffering from SARS-CoV-2 pneumonia.

As such, it is tempting to speculate that risk classification of patients according to the CAC-DRS Score might correlate with disease severity of SARS-CoV-2 pneumonia and facilitate classification of patients into different risk groups. Thus, the purpose of this study was to quantitatively assess pulmonary involvement and to evaluate the prognostic value of the CAC-DRS reporting system in patients with SARS-CoV-2 pneumonia.

METHODS

The institutional ethical review board approved this retrospective study, which complies with the Declaration of Helsinki. Written informed consent was waived.

Study Population

A total of 158 patients with confirmed SARS-CoV-2 on reverse transcription-polymerase chain reaction and

corresponding clinical symptoms who had undergone non-contrast chest CT scans between January 2020 and September 2021 were candidates for study inclusion. Indications to perform non-contrast CT scans included severity assessment of SARS-CoV-2 pneumonia, searching after complications of SARS-CoV-2 due to persistent symptoms, and position control of implanted central venous catheters. The study was performed at two sites, the University Hospital Frankfurt and the University Hospital Messina. Searching for appropriate patients was performed on PACS (picture archiving and communication system) and internal patient database using the following terms: ‘SARS-CoV-2’, ‘COVID-19’ and ‘pneumonia’. Exclusion criteria were artefacts (e.g., due to dorsal instrumentation, insufficient image quality, or excessive pleural effusion), implanted coronary stents, previous coronary artery bypass grafting, and patient age <18 years.

Clinical and Laboratory Data

Data about demographics, symptoms, laboratory, hospital stay, and outcomes were obtained from medical reports. Extracted laboratory values included hs-Troponin T (hs-TnT), N-terminal pro brain natriuretic peptide (NT-proBNP), leucocytes, C-reactive protein, and procalcitonin. All values were determined at the peak of symptoms and analyzed with regards to possible correlations with the automated quantification of lung opacities and coronary plaque burden. Follow-up was performed by extracting outcome information from all available databases, including internal hospital files and data from collaborating clinics, and analyzed for the endpoint death. Follow-up time was not limited to a defined number of days and comprised all available information.

CT Scan Protocol

Non-contrast chest CT scans were conducted in craniocaudal scan direction on a third-generation dual-source dual-energy CT scanner (Somatom Force; Siemens Healthineers, Forchheim, Germany), and on a conventional multislice CT scanner (Somatom Definition AS; Siemens Healthineers, Forchheim, Germany). All scans were not ECG-gated and performed using a conventional protocol with the following parameters: 120 kV, 70 mAs 0.6 mm slice thickness, and 1 mm collimation.

Image Reconstruction and Evaluation

For the evaluation of SARS-CoV-2 pneumonia, axial, coronal, and sagittal (slice thickness of 1 mm, interscan spacing 1.5 mm) images were reconstructed from each CT scan. Three-dimensional visualization and quantification of SARS-CoV-2-related lung abnormalities were performed using a previously described software prototype (6). Briefly, the software allowed for automated segmentation and calculation of pneumonic densities, such as consolidations and ground glass opacities, which are finally displayed as Opacity Score with a

corresponding Lung Severity Score. In this context, the maximum density of opacities was defined by a threshold of -200 Hounsfield Units (HU). The software was developed and constructed for research purposes by using algorithms based on artificial intelligence (6,17). The Opacity Score ranged from 0–20 relative units (RU), representing all affected areas from both lungs. A value of zero indicated no pulmonary involvement, while an Opacity Score of 20 was associated with the maximal pulmonary opacification of both lungs. Each automated examination of lung opacities was proven and confirmed by two radiologists (I.Y., board-certified radiologist with 5 years of experience, and M.H.A., board-certified radiologist with 6 years of experience) in consensus reading sessions. Automated postprocessing of lung opacities is illustrated in Figure 1 showing examples of axial and coronal grayscale CT scans from a 51-year-old male with SARS-CoV-2 pneumonia at a moderate level (9.4 RU).

For the assessment of CAC, images were reconstructed with the following parameters: section thickness of 3 mm, interscan spacing of 1.5 mm, and a field of view (FOV) of 18 cm limited to the heart. CAC-DRS categories were subjectively assessed by applying a visual score as well as objectively by using a HU-based quantitative score (referred to as visual and quantitative analysis in the manuscript). Regarding the visual assessment of coronaries, one radiologist (S.S.M., board-certified radiologist with 8 years of experience) analyzed each coronary artery for the presence and extent of CAC using a visual scale ranging from V0 to V3. Hereby, a CAC-DRS category of V0 indicates no CAC with very low risk, a score of V1 mild coronary affection with mildly increased risk, V2 moderate CAC with moderately increased risk, and a score of V3 severe coronary calcium with high risk (11). The quantitative HU-based score represents a semi-automated tool to objectively assess the extent of CAC, where 0 is assigned to a CAC-DRS category of A0, 1–99 to

A1, 100–299 to A2, and > 300 to A3 (11). For the quantitative evaluation of CAC, the region of interest was manually placed in each coronary artery with subsequent automatically calculated CAC for each coronary and in total by summation of all scores, as previously described (18–21). Software-based automated calculation was performed by applying a threshold of 130 HU within ≥ 3 contiguous pixels, resulting in a minimum area of 1.05 mm^2 .

All postprocessing steps were performed on a commercially available workstation (syngo.via, version VB10B; Siemens Healthineers, Forchheim, Germany). The three radiologists could freely modify window settings and scroll through the whole stack of CT scans. No case required manual adjustment of opacity areas that were not correctly recognized by the automated software prototype. After each examination, overall assessment time of image analysis was noted.

Statistical Analysis

Commercially available software was used for statistical analysis (MedCalc for Windows, Version 13; MedCalc, Ostend, Belgium). Normal distribution of datasets was assessed by using the Kolmogorov-Smirnov and Shapiro-Wilk test. Results are expressed as mean \pm standard deviation (SD), count (percentages), or median (interquartile range, IQR), where appropriate. Comparisons between continuous variables were conducted using one-way ANOVA, chi-square statistic test, or two-tailed Student's *t*-test, where appropriate. Pearson's correlation was used to test the association between SARS-CoV-2 opacities and clinical or laboratory parameters. An *r* value of less than 0.40, 0.41–0.60, 0.61–0.80 and > 0.80 was considered as poor, moderate, strong, and very strong, respectively. Cox regression analysis was performed to explore independent factors associated with CAC-DRS Score of patients with SARS-CoV-2 considering all

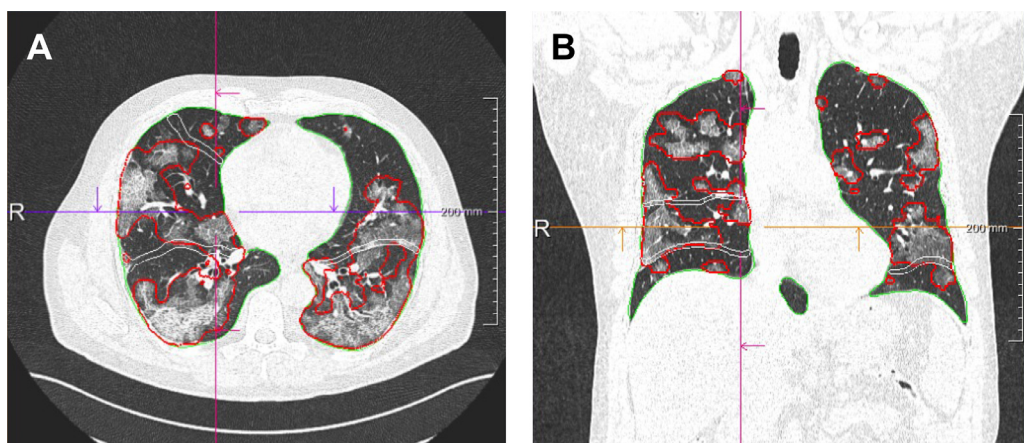


Figure 1. Representative axial (A) and coronal (B) grayscale CT images obtained from a 51-year-old male with SARS-CoV-2 pneumonia after postprocessing of lung opacities using the software prototype on a commercially available workstation (syngo.via, version VB10B; Siemens Healthineers, Forchheim, Germany). The software was capable of providing a colored visualization of lung opacities (volume-rendering technique, VRT), illustrated as red circumscribed areas of lung parenchyma. Abbreviations: SARS-CoV-2, severe acute respiratory syndrome coronavirus type 2. VRT, volume-rendering technique (Color version of figure is available online).

parameters. Those with $p < 0.05$ in univariate analysis were transferred into the multivariate linear regression model. Receiver operating characteristic (ROC) curves were plotted and areas under the curves (AUCs) were calculated together with their 95% confidence intervals (95% CI). The diagnostic performance was calculated for every single score as well as for the combination of them, which was defined as the Composite Score. Interrater agreement was assessed by using weighted κ statistics (22), where values of < 0.20 , $0.21-0.40$, $0.41-0.60$, $0.61-0.80$, and > 0.80 were regarded as none to slight, fair, moderate, substantial, and excellent, respectively. A $p < 0.05$ was considered statistically significant.

RESULTS

A total of 142 patients (58 ± 16 years; range, 21–87), consisting of 85 men (57 ± 14 years; range, 28–81) and 57 women (59 ± 18 years; range, 21–87), were included in this study. The time gap between admission, clinical evaluation, laboratory test sampling, and CT scanning was 18 ± 4 hours for all enrolled patients. 16 patients had previously been excluded due to large pleural effusion (11 patients), dorsal instrumentation (3 patients), and patient age < 18 years (2 patients) (Fig 2). Overall mean body mass index (BMI) was $27 \text{ kg/m}^2 \pm 4$, ranging between 18 and 37 kg/m^2 ($p = 0.0193$).

Risk factors of patients with SARS-CoV-2 included arterial hypertension (44%), a positive family history of cardiovascular disease (33%), diabetes mellitus (24%), hypercholesterolemia (20%), and smoking (19%). Most observed symptoms consisted of dyspnea (76%), cough (65%), fever (60%), headache (32%), and less prevalent gastrointestinal symptoms, such as diarrhea (16%).

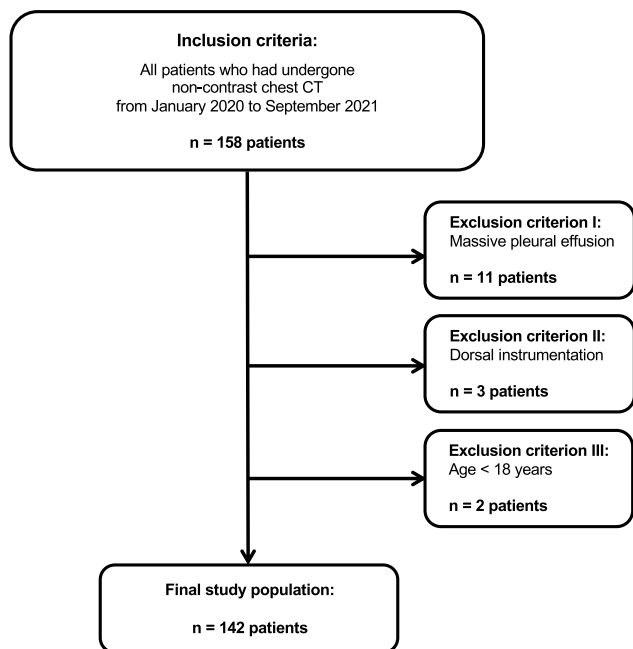


Figure 2. Illustration of patient inclusion (n=142).

Regarding outcome, 53 patients (37%) required intensive care, of whom 28 died after a mean duration of 18 ± 11 days (range, 4–51). Of all patients requiring intensive care treatment, 41 patients (77%) had ≥ 2 cardiovascular risk factors. Interestingly, the need for ventilation was positively associated with the extent of coronary plaque burden (54% of patients with CAC-DRS Score of 3 vs. 15% with a Score of 0). The rate of comorbidities was significantly lower in patients who survived (23% vs. 77%, $p = 0.036$), particularly with regards to arterial hypertension, family history, and smoking. Of the 28 deaths, 21 patients died because of respiratory failure, 6 patients due to cardiogenic shock, and 1 patient due to gastric hemorrhage. Baseline characteristics of patients with SARS-CoV-2 are depicted in Table 1.

Characteristics of Imaging Parameters

Characteristics of imaging scores are displayed in Table 2. Opacities were present in all CT scans with an Opacity Score ranging from 0.6 to 19.7 RU. The overall Opacity Score comprising both lungs was 7.5 ± 4.5 RU, where patients with a visual CAC-DRS Score of V3 (12.4 ± 3.2 RU) revealed higher opacities than patients with a score of V2 (8.5 ± 2.9 RU), V1 (5.4 ± 2.9 RU), and V0 (2.9 ± 1.9 RU) (all $p < 0.0001$). Interrater agreement between the two raters was excellent for the assessment of lung opacities ($\kappa = 0.94$ [95% CI, 0.89 to 0.99]). In terms of percentual affection, $31.6 \pm 26.2\%$ of both lungs showed pulmonary consolidations associated with SARS-CoV-2 pneumonia. Overall assessment of lung opacities as well as the visual and quantitative CAC-DRS Score took 6 minutes on average for each CT scan (range, 5–7 minutes).

The quantitative HU-based CAC-DRS Score differed significantly between CAC-DRS categories from 0 to 3, with values of 695 ± 408 for category A3, 190 ± 69 for A2, 53 ± 36 for A1, and a score of 0 for the category A0 ($p < 0.0001$).

A case of SARS-CoV-2 pneumonia is depicted in Figure 3, showing a 41-year-old man with mild lung manifestation (Opacity Score of 4.3 RU) and a CAC-DRS Score of 0. Figure 4 shows a 67-year-old male with severe SARS-CoV-2 pneumonia and extensive ground glass opacities and consolidations 8 hours after admission (Opacity Score of 17.6 RU) and a CAC-DRS Score of 3.

Correlation Analysis

Visual and quantitative evaluation of calcified plaque area were highly correlated to the Opacity Score ($r = 0.81$, 95% CI 0.76–0.86 for the visual, and $r = 0.83$, 95% CI 0.77–0.89 for the quantitative CAC-DRS Score, respectively; $p < 0.0001$), without significant difference between the two correlation coefficients ($p = 0.3504$). Bivariate correlation analysis revealed not only a significant correlation of the Opacity Score with the visual CAC-DRS Score, but also with hs-TnT ($r = 0.58$, 95% CI 0.51–0.65; $p < 0.0001$) and parameters of inflammatory response like C-reactive

TABLE 1. Baseline Characteristics of The Study Cohort (n=142) According to the CAC-DRS Score.

Variables	Overall (n=142; 100%)	CAC-DRS 0 (n=33; 23%)	CAC-DRS 1 (n=34; 24%)	CAC-DRS 2 (n=36; 25%)	CAC-DRS 3 (n=39; 28%)	p-value
Demographics						
Age (years) ± SD (range)	58 ± 16 (21-87)	56 ± 16	58 ± 15	60 ± 17	59 ± 16	0.7516
Males (n)	85 (60%)	18 (55%)	24 (71%)	20 (56%)	23 (60%)	
Females (n)	57 (40%)	15 (45%)	10 (29%)	16 (44%)	16 (41%)	
Body mass index (kg/m ²) ± SD (range)	27 ± 4 (18-37)	26 ± 5	26 ± 3	27 ± 3	28 ± 4	0.0193
Vital signs						
Heart rate (bpm) ± SD (range)	77 ± 15 (51-119)	78 ± 17	75 ± 14	76 ± 13	81 ± 15	0.3117
Systolic blood pressure (mmHg) ± SD (range)	133 ± 26 (90-190)	132 ± 22	137 ± 24	134 ± 25	129 ± 30	0.6011
Diastolic blood pressure (mmHg) ± SD (range)	84 ± 13 (50-118)	82 ± 12	86 ± 13	84 ± 15	83 ± 13	0.7508
Risk factors						
Arterial hypertension (n)	62 (44%)	9 (27%)	12 (35%)	17 (47%)	24 (61%)	
Family history (n)	47 (33%)	8 (24%)	9 (27%)	13 (36%)	17 (44%)	
Diabetes mellitus (n)	34 (24%)	5 (15%)	7 (21%)	12 (33%)	10 (26%)	
Hypercholesterolemia (n)	28 (20%)	6 (18%)	6 (18%)	7 (19%)	9 (23%)	
Smoking (n)	27 (19%)	4 (12%)	4 (12%)	6 (17%)	13 (33%)	
Clinical course						
Length of hospital stay (d) ± SD (range)	12 ± 12 (0-79)	5 ± 5	10 ± 9	11 ± 9	19 ± 18	<0.0001
Length of intensive care (d) ± SD (range)	16 ± 15 (1-79)	4 ± 5	10 ± 8	13 ± 9	25 ± 20	0.0046
Need for intensive care (n)	53 (37%)	6 (18%)	10 (29%)	16 (44%)	21 (54%)	
Need for ventilation (n)	52 (37%)	5 (15%)	10 (29%)	16 (44%)	21 (54%)	
Number of deaths (n)	28 (20%)	3 (9%)	4 (12%)	7 (19%)	14 (36%)	

Abbreviations: CAC-DRS, Coronary Artery Calcium Data and Reporting System; SD, standard deviation.

protein ($r=0.53$, 95% CI 0.49-0.57; $p<0.0001$), procalcitonin ($r=0.59$, 95% CI 0.54-0.64), and leucocytes ($r=0.57$, 95% CI 0.51-0.63; $p<0.0001$). Median plasma

hs-cTnT concentration was 11 pg/mL (IQR 6, 44) comprising all patients (n=142). Patients with a CAC-DRS Score of 3 (19 pg/mL, IQR 8, 74) showed higher levels

TABLE 2. Findings derived from quantitative HU-based CAC-DRS assessment and Opacity Score in patients with SARS-CoV-2 pneumonia.

Imaging Parameter	Opacity Score (RU, 1-20)	95% CI	p-value (vs. CAC-DRS 3)	Quantitative Score (HU)	95% CI	p-value (vs. CAC-DRS 3)
CAC-DRS Score (0-3)						
0	2.9 ± 1.9	[2.3-3.6]	<0.0001	0	-	<0.0001
1	5.4 ± 2.9	[4.4-6.4]	<0.0001	53 ± 36	[40-65]	<0.0001
2	8.5 ± 2.9	[7.6-9.5]	<0.0001	190 ± 69	[166-213]	<0.0001
3	12.4 ± 3.2	[11.4-13.5]	-	695 ± 408	[561-826]	-
Overall	7.5 ± 4.5	[6.8-8.3]	-	251 ± 355	[192-310]	-

Abbreviations: RU, relative unit; CI, confidence interval; CAC-DRS, Coronary Artery Calcium Data and Reporting System; HU, Hounsfield Unit; SARS-CoV-2, severe acute respiratory syndrome coronavirus type 2.

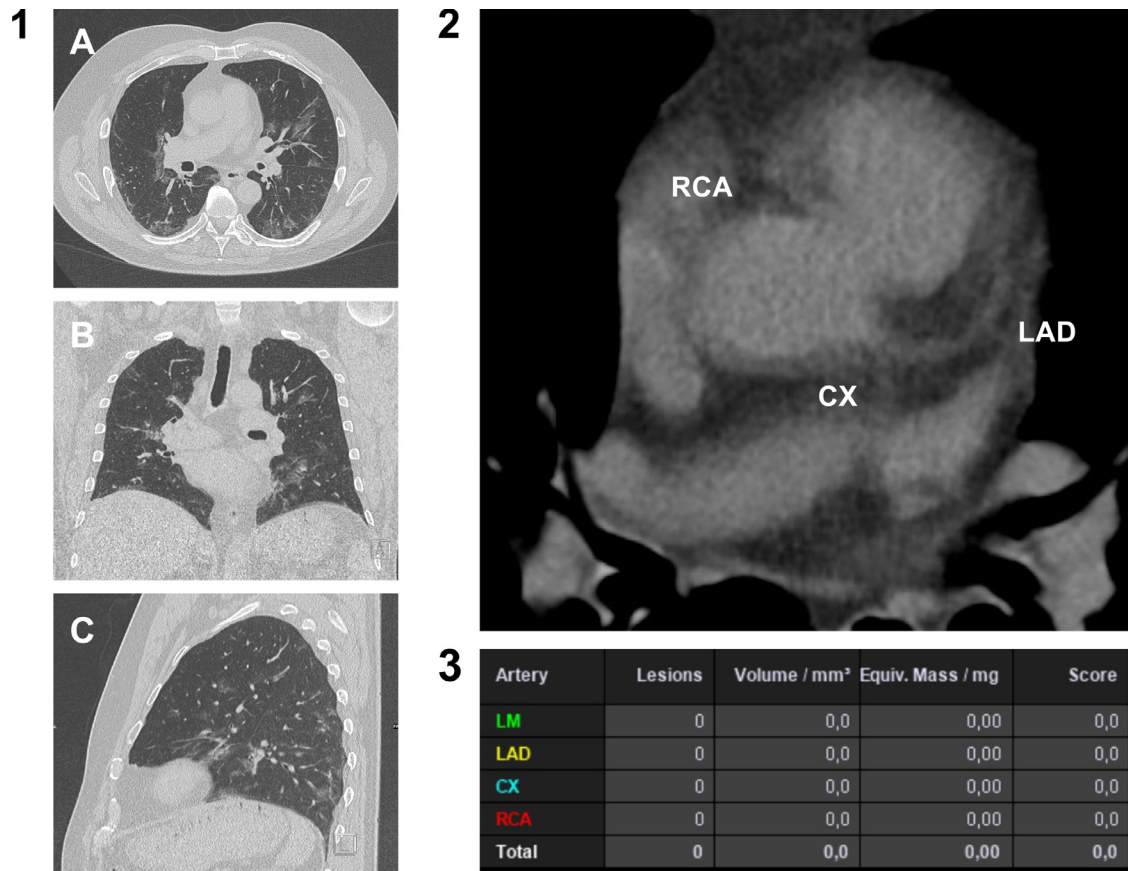


Figure 3. The images illustrate a case of a 41-year-old man with confirmed SARS-CoV-2 pneumonia, initially presenting with moderate fever, cough, and limb pain. Due to persistent symptoms, a CT scan was performed after admission (1). Lung parenchyma was typically affected by multiple small patchy areas of ground glass opacities, mainly peripherally located as shown in axial (1A), coronal (1B), and sagittal (1C) gray-scale CT images. The overall Opacity Score was found to be at 4.3 RU. Hospital stay was 5 days in total without the need for intensive care treatment. Coronary arteries (2) were not affected by calcified coronary plaques corresponding to a CAC-DRS category of 0 based on both visual and quantitative HU-based assessment (3). Abbreviations: SARS-CoV-2, severe acute respiratory syndrome coronavirus type 2. RU, relative unit. CAC-DRS, Coronary Artery Calcium Data and Reporting System. RCA, right coronary artery. LAD, left anterior descending. Cx, left circumflex. LM, left main (Color version of figure is available online).

of hs-cTnT as compared to patients with a score of 0 (8 pg/mL, IQR 6, 9; $p=0.0375$). Parameters of clinical course were also positively associated with the degree of ground glass opacities in CT, such as the need for intensive care treatment ($r=0.43$, 95% CI 0.29 to 0.58; $p<0.0001$), length of intensive care treatment ($r=0.76$, 95% CI 0.65-0.87; $p<0.0001$), and mortality ($r=0.52$, 95% CI 0.41-0.63; $p<0.0001$).

Discriminative Value of Coronary Plaque Burden Based on the CAC-DRS Score

The diagnostic performance to discriminate patients with a fatal outcome was good for the Opacity Score with an AUC value of 0.870 (95% CI, 0.80-0.92), fair for the quantitative CAC-DRS Score (0.785, 95% CI 0.71-0.85), and poor for the visual CAC-DRS Score (0.679, 95% CI 0.60-0.76). Adding the extent of coronary calcification as derived from the visual and quantitative CAC-DRS Score to the Opacity

Score increased the AUC significantly by 0.0678 (AUC 0.938, 95% CI 0.89-0.97, standard error 0.0363; $p=0.0404$), which is expressed as the Composite Score in Figure 5.

Combining the Opacity Score with both CAC-DRS Scores allowed for a good discrimination of patients that required intensive care treatment with an AUC of 0.801 (95% CI 0.77-0.83).

Prognostic Role of the CAC-DRS Score

Patients were followed up over a time interval of 129 ± 72 days for the endpoint death. A total of 14 patients were lost to follow-up. Visual and quantitative CAC-DRS Scores were positively associated with all-cause mortality. In this context, patients with a CAC-DRS Score of 3 showed higher mortality than patients with a Score of 0 (Score 3 vs. 0: hazard ratio [HR], 4.85 [95% CI 1.69-13.92]; $p=0.0101$) (Fig 6).

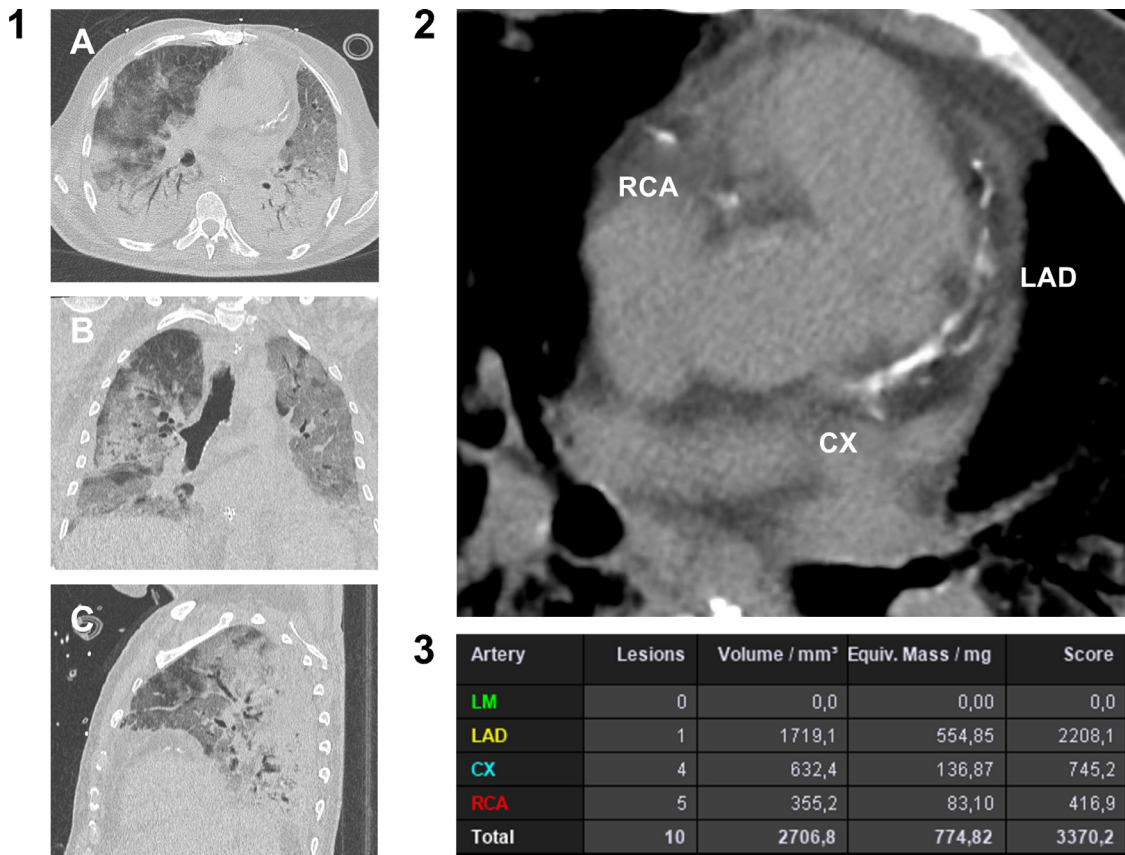


Figure 4. Case of a 67-year-old male patient with severe SARS-CoV-2 pneumonia, corresponding to an Opacity Score of 17.6 RU (1). Extensive affection of lung parenchyma on both sides was visible on axial (1A), coronal (1B), and sagittal (1C) grayscale CT images. Coronary sclerosis affected all three vessels showing pronounced plaque formation. CAC values were increased, corresponding to a CAC-DRS category of 3 on visual and HU-based quantitative coronary plaque assessment (3). Abbreviations: SARS-CoV-2, severe acute respiratory syndrome coronavirus type 2. RU, relative unit. PCI, percutaneous intervention. LAD, left anterior descending. CAC, coronary artery calcium. CAC-DRS, Coronary Artery Calcium Data and Reporting System. RCA, right coronary artery. Cx, left circumflex. LM, left main (Color version of figure is available online).

Using Cox regression models, the visual and quantitative CAC-DRS Scores have been shown to provide independent prognostic information for the endpoint death ($p=0.0016$ and $p<0.0001$, respectively). Results remained significant after adjustment for potential confounders that have been identified in the univariate analysis (Table 3).

Adding either the Opacity- or quantitative CAC-DRS Score to visual CAC-DRS assessment increased the χ^2 value from 10 to 52 ($p<0.0001$) and from 10 to 22 ($p<0.0001$), respectively.

DISCUSSION

This study found that coronary plaque burden according to the CAC-DRS Score was strongly associated with the extent of SARS-CoV-2 pneumonia (correlation coefficient of at least $r=0.81$, 95% CI 0.76-0.86), and provided independent prognostic information on all-cause mortality ($p\leq 0.0016$). Moreover, incorporating the degree of coronary plaque burden and pulmonary involvement into clinical decision making revealed great potential to discriminate patients with fatal

outcome from a mild course of disease (AUC 0.938, 95% CI 0.89-0.97), and the requirement for intensive care treatment (AUC 0.801, 95% CI 0.77-0.83).

Cardiovascular comorbidities are common in patients with SARS-CoV-2 (4) bearing the risk for adverse outcome due to complex and incompletely understood pathological mechanisms. In this study, 44% of patients had at least one cardiovascular risk factor, in line with previous reports (2,3,23,24). The prevalence of coronary artery disease increased over the past decade, partly attributable to demographic changes with gradual ageing of the population as well as lifestyle choices such as smoking and obesity due to unhealthy diet. Several algorithms have been proposed aiming at assisting physicians in risk stratification of patients. Determination of CAC on CT scans was found to be a robust predictor of cardiovascular events in asymptomatic patients, especially in those at intermediate risk (12). According to the 2017 Expert Consensus Statement from the Society of Cardiovascular Computed Tomography (SCCT), measurement of CAC is recommended in case of an atherosclerotic cardiovascular disease 10-year risk ranging between 5% and 20% as well as in

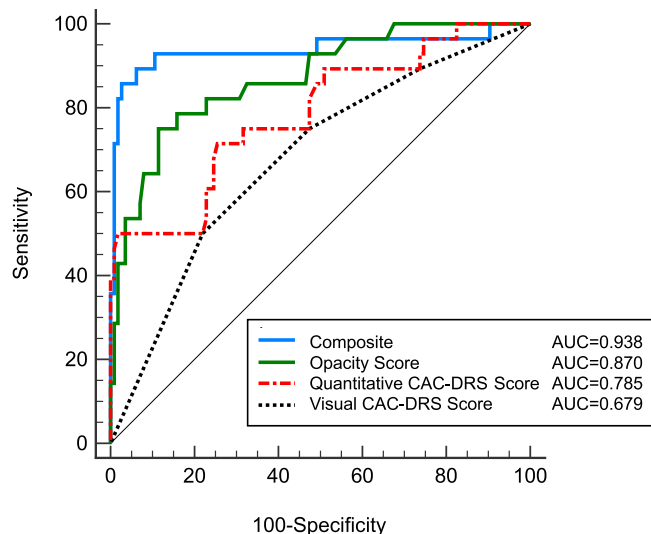


Figure 5. Receiver operating characteristic (ROC) curve analysis showing the diagnostic performance of the Opacity- and CAC-DRS Scores for prediction of mortality in patients with SARS-CoV-2 pneumonia. ROC curve is depicted in blue (composite ROC-curve combining all three scores), green (Opacity Score), red (quantitative CAC-DRS Score), and black (visual CAC-DRS Score). Abbreviations: ROC, receiver operating characteristic. SARS-CoV-2, severe acute respiratory syndrome coronavirus type 2. CAC-DRS, Coronary Artery Calcium Data and Reporting System (Color version of figure is available online).

selected patients showing a family history of premature coronary artery disease at values inferior to 5% [12]. Clear management strategies are of particular importance since, as the SARS-CoV-2 pandemic revealed, even mild cases are at increased risk for adverse outcomes.

Pneumocytes are primarily vulnerable for SARS-CoV-2, which makes the pulmonary status of patients to the principal determinant of disease severity and outcome (25). As early abnormalities remain often hidden on chest X-rays with a considerable number of false negatives, other imaging strategies were investigated for a more sensitive capturing of early parenchymal changes (26). Previous research extensively assessed the role of thin-section chest-CT scans for diagnostic workup and outcome prediction of SARS-CoV-2 pneumonia (27). In this context, Mader et al. evaluated a fully automated software prototype for the quantification of lung opacities associated with SARS-CoV-2 and found strong correlations with clinical outcome and laboratory parameters of inflammation (6). Yang et al. reported on a semiquantitative method for assessing severity of SARS-CoV-2 pneumonia on chest CT images, which enabled successful rule-out of

severe pulmonary involvement of disease with a high negative predictive value of 96.3% (28). Other studies found similar radiological manifestation patterns using the semiquantitative assessment method, such as peripheral distribution, crazy-paving pattern, involvement of lower parenchymal areas of the lung, or reticulation patterns after recovery (7,29-32). The concept of standardized and structured reporting of diseases through comprehensive documents has become increasingly important to provide data collection from different international centers and facilitate uniform patient management by closing knowledge gaps about outcome data across all populations (11).

Our study clearly demonstrated that the Composite Score of lung opacities and the degree of coronary plaque burden according to the visual or quantitative HU-based CAC-DRS Score was able to predict all-cause mortality during a follow-up period of 129 ± 72 days. The predictive value has to be underlined as the most striking aspect of our study results. In this context, quantitative CAC assessment based on measurement of Hounsfield Units allowed for a slightly more precise outcome prognosis than the visual assessment of coronary

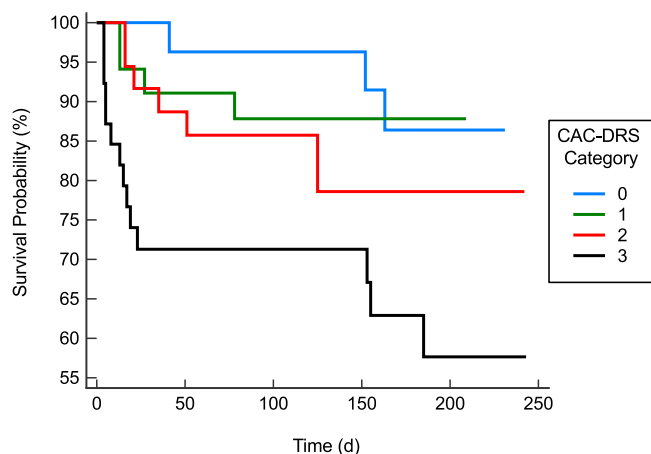


Figure 6. Kaplan-Meier curve showing overall cumulative survival probability according to the CAC-DRS Score (all $p < 0.05$). Abbreviations: CAC-DRS, Coronary Artery Calcium Data and Reporting System (Color version of figure is available online).

TABLE 3. Predictors of progression to severe disease outcome in univariate and multivariate models. Cox-regression models of patients with coronary artery disease for the occurrence of death.

Model	Endpoint (death)				
	b	SE	Exp(b)	95% CI of Exp(b)	p-value
Unadjusted Model 1	0.5730	0.1931	1.7737	1.2148-2.5897	0.0016
Adjusted Model 2	0.4215	0.0662	1.5242	1.3387-1.7354	<0.0001
Adjusted Model 3	0.0013	0.0003	1.0013	1.0007-1.0019	<0.0001
Adjusted Model 4	0.5184	0.0919	1.6793	1.4025-2.0107	<0.0001
Adjusted Model 5	0.5382	0.0966	1.7129	1.4176-2.0698	<0.0001

Model 1: unadjusted model for basic visual CAC-DRS Score. Model 2: additionally adjusted by Opacity Score. Model 3: additionally adjusted by the quantitative CAC-DRS Score. Model 4: additionally adjusted by Opacity Score and the quantitative CAC-DRS Score. Model 5: additionally adjusted by Opacity Score, quantitative CAC-DRS Score, and age.

Abbreviations: CAC-DRS, Coronary Artery Calcium Data and Reporting System; b, regression coefficient. Exp(b), ratio of hazard rates; CI, confidence interval; SE, standard error. Variables that did not reach univariate significance: sex ($p=0.5890$), hs-TnT ($p=0.1803$), diabetes mellitus ($p=0.1834$), NT-proBNP ($p=0.0678$). Variables that reached univariate significance: age ($p<0.0001$), C-reactive protein ($p=0.0175$), leucocytes ($p=0.0262$), arterial hypertension ($p=0.0319$), hypercholesterolemia ($p=0.0471$), family history ($p=0.0271$).

calcifications ($p<0.0001$ vs. $p=0.0016$, respectively). High coronary plaque burden was associated with more severe pulmonary manifestations of SARS-CoV-2 pneumonia, expressed as percentual affection of both lungs. In accordance with previous studies (3-5,8,14-16,33) patients with coronary artery disease were prone to a complicated clinical course, including the need for intensive care treatment, an increased risk for mechanical ventilation, the use of vasoactive agents, and higher mortality. A high CAC-DRS score in patients with SARS-CoV-2 pneumonia may therefore reflect an ongoing inflammatory cascade with susceptibility to complications and higher mortality. Dillinger et al. described first that the extent of coronary artery calcifications is associated with a worse outcome in hospitalized patients with COVID-19 using Agatston scoring on non-cardiac gated CT chest (14). Although the evaluation of CAC is traditionally conducted using ECG synchronization, our findings suggest a good correlation between CAC and outcome using non-gated chest CT scans in accordance with previous publications (15,18-21,34,35). Regarding possible cardiac motion artifacts in chest CT scans without ECG synchronization, our included examinations were not significantly affected by motion artifacts facilitating accurate evaluation of coronary plaque burden.

In a clinical context, the combined assessment of CAC and pulmonary involvement of SARS-CoV-2 consolidations in non-dedicated, non-gated chest CT scans adds incremental prognostic information allowing for cardiovascular risk stratification without additional costs. Therefore, this combined approach may represent an elegant method in daily clinical routine to save radiation exposure by avoiding specific cardiac CT scans. Furthermore, patient comfort can considerably be increased obviating the need for repeated transport of immobile patients.

CAC scoring is a simple, highly reproducible tool for assessment of atherosclerotic diseases providing tailored personalized therapy (11,13). It offers a direct objective assessment of coronary plaque burden and may therefore assist in evaluating the individual optimal therapeutic guidance. In combination with the reported Opacity Score, this novel

assessment tool may especially be useful for intermediate-risk patients with SARS-CoV-2 pneumonia who fall into grey zones where frequently only epidemiological or empirical data are used to provide further guidance in therapy.

Given its high predictive value, CAC scanning might motivate patients to change their lifestyle and to raise their awareness regarding potential complications, such as myocardial infarction. In a prospective randomized trial with 2,137 middle-aged study participants and a meta-analysis of 11,256 patients from six studies, randomization to CAC scanning was associated with superior control of cardiovascular risk factors and a higher likelihood of continuation of cardioprotective medical therapy and lifestyle modification (36,37). However, CAC scanning might not only be useful in estimating net benefits from preventive pharmaceutical treatment, but also in providing therapeutic goals and subsequent regulation of treatment intensity in patients suffering from SARS-CoV-2 pneumonia.

This study had several limitations. First, our examinations were conducted as a retrospective study with a limited number of patients. Validation of our study findings in larger patient cohorts is required. Second, the automated determination of Opacity Score using a software prototype assumed the extent of pulmonary opacities as a surrogate for the severity of SARS-CoV-2 pneumonia without histological confirmation. Third, the automated evaluation of chest CT scans was performed at different stages of SARS-CoV-2 pneumonia, which potentially has led to over- or underestimation of disease severity. Fourth, laboratory parameters were collected only at the peak of symptoms without considering dynamic changes over time. Fifth, our study findings are currently only reproducible on a dedicated vendor-specific CT setup with the possibility for postprocessing of chest CT scans. Therefore, our results may not be transferable to devices and technologies merchandised by other manufacturers. Sixth, CT scans were performed during the peak of SARS-CoV-2 pneumonia which possibly has led to inclusion of more patients with severe disease than those with milder symptoms.

Finally, though we have thoroughly checked all databases for follow-up data, 14 patients were lost to follow-up.

To summarize, the present study shows that the degree of coronary artery plaque burden based on the CAC-DRS classification correlates well with the severity of SARS-CoV-2 pneumonia and provides independent prognostic information on all-cause mortality. Furthermore, the CAC-DRS classification facilitates high diagnostic performance to discriminate patients at risk for complicated courses of disease from those with mild outcomes. Therefore, measurement of CAC in non-gated chest CT scans of patients with SARS-CoV-2 pneumonia may assist physicians in clinical decision making by allocating patients to a certain risk category.

FUNDING

This research did not receive any specific grant from funding agencies in the public, commercial, or non-for-profit sectors.

REFERENCES

1. Rehman H, Ahmad MI. COVID-19: a wreak havoc across the globe. *Arch Physiol Biochem* 2020. doi:10.1080/13813455.2020.1797105:1-13.
2. Huang D, Lian X, Song F, et al. Clinical features of severe patients infected with 2019 novel coronavirus: a systematic review and meta-analysis. *Ann Transl Med* 2020; 8:576.
3. Srivastava K. Association between COVID-19 and cardiovascular disease. *Int J Cardiol Heart Vasc* 2020; 29:100583.
4. Wei JF, Huang FY, Xiong TY, et al. Acute myocardial injury is common in patients with COVID-19 and impairs their prognosis. *Heart* 2020; 106:1154-1159.
5. Gupta YS, Finkelstein M, Manna S, et al. Coronary artery calcification in COVID-19 patients: an imaging biomarker for adverse clinical outcomes. *Clin Imaging* 2021; 77:1-8.
6. Mader C, Bernatz S, Michalik S, et al. Quantification of COVID-19 opacities on Chest CT - evaluation of a fully automatic AI-approach to noninvasively differentiate critical versus noncritical patients. *Acad Radiol* 2021; 28:1048-1057.
7. Zhang R, Ouyang H, Fu L, et al. CT features of SARS-CoV-2 pneumonia according to clinical presentation: a retrospective analysis of 120 consecutive patients from Wuhan city. *Eur Radiol* 2020; 30:4417-4426.
8. Scoccia A, Gallone G, Cereda A, et al. Impact of clinical and subclinical coronary artery disease as assessed by coronary artery calcium in COVID-19. *Atherosclerosis* 2021; 328:136-143.
9. Eghtedari M, Chong A, Rakow-Penner R, et al. Current status and future of BI-RADS in multimodality imaging, from the AJR special series on radiology reporting and data systems. *AJR Am J Roentgenol* 2021; 216:860-873.
10. An JY, Unsrdorfer KML, Weinreb JC. BI-RADS, C-RADS, CAD-RADS, LI-RADS, Lung-RADS, NI-RADS, O-RADS, PI-RADS, TI-RADS: Reporting and data systems. *Radiographics* 2019; 39:1435-1436.
11. Hecht HS, Blaha MJ, Kazerooni EA, et al. CAC-DRS: Coronary artery calcium data and reporting system. an expert consensus document of the society of cardiovascular computed tomography (SCCT). *J Cardiovasc Comput Tomogr* 2018; 12:185-191.
12. Hecht H, Blaha MJ, Berman DS, et al. Clinical indications for coronary artery calcium scoring in asymptomatic patients: expert consensus statement from the society of cardiovascular computed tomography. *J Cardiovasc Comput Tomogr* 2017; 11:157-168.
13. Arnett DK, Blumenthal RS, Albert MA, et al. 2019 ACC/AHA guideline on the primary prevention of cardiovascular disease: a report of the American college of cardiology/American heart association task force on clinical practice guidelines. *J Am Coll Cardiol* 2019; 74:e177-e232.
14. Dillinger JG, Benmessaoud FA, Pezel T, et al. Coronary artery calcification and complications in patients with COVID-19. *JACC Cardiovasc Imaging* 2020; 13:2468-2470.
15. Fervers P, Kottlors J, Grosse Hokamp N, et al. Coronary artery calcification on low-dose chest CT is an early predictor of severe progression of COVID-19-A multi-center, multi-vendor study. *PLoS One* 2021; 16:e0255045.
16. Nair AV, Kumar D, Yadav SK, et al. Utility of visual coronary artery calcification on non-cardiac gated thoracic CT in predicting clinical severity and outcome in COVID-19. *Clin Imaging* 2021; 74:123-130.
17. Chaganti S, Grenier P, Balachandran A, et al. Automated quantification of CT patterns associated with COVID-19 from Chest CT. *Radiol Artif Intell* 2020; 2:e200048.
18. Suh YJ, Lee JW, Shin SY, et al. Coronary artery calcium severity grading on non-ECG-gated low-dose chest computed tomography: a multiple-observer study in a nationwide lung cancer screening registry. *Eur Radiol* 2020; 30:3684-3691.
19. Takx RA, de Jong PA, Leiner T, et al. Automated coronary artery calcification scoring in non-gated chest CT: agreement and reliability. *PLoS One* 2014; 9:e91239.
20. Isgum I, Prokop M, Niemeijer M, et al. Automatic coronary calcium scoring in low-dose chest computed tomography. *IEEE Trans Med Imaging* 2012; 31:2322-2334.
21. Shin JM, Kim TH, Kim JY, et al. Coronary artery calcium scoring on non-gated, non-contrast chest computed tomography (CT) using wide-detector, high-pitch and fast gantry rotation: comparison with dedicated calcium scoring CT. *J Thorac Dis* 2020; 12:5783-5793.
22. Landis JR, Koch GG. The measurement of observer agreement for categorical data. *Biometrics* 1977; 33:159-174.
23. Blankstein R. The impact of the COVID-19 pandemic on cardiac CT. *J Cardiovasc Comput Tomogr* 2020; 14:209-210.
24. Li B, Zhang S, Zhang R, et al. Epidemiological and clinical characteristics of COVID-19 in children: a systematic review and meta-analysis. *Front Pediatr* 2020; 8:591132.
25. Lu R, Zhao X, Li J, et al. Genomic characterization and epidemiology of 2019 novel coronavirus: implications for virus origins and receptor binding. *Lancet* 2020; 395:565-574.
26. Rubin GD, Ryerson CJ, Haramati LB, et al. The Role of chest imaging in patient management during the COVID-19 pandemic: a multinational consensus statement from the fleischner society. *Chest* 2020; 158:106-116.
27. Pontone G, Scafuri S, Mancini ME, et al. Role of computed tomography in COVID-19. *J Cardiovasc Comput Tomogr* 2021; 15:27-36.
28. Yang R, Li X, Liu H, et al. Chest CT severity score: an imaging tool for assessing severe COVID-19. *Radiol Cardiothorac Imaging* 2020; 2:e200047.
29. Duan YN, Qin J. Pre- and posttreatment Chest CT findings: 2019 novel coronavirus (2019-nCoV) pneumonia. *Radiology* 2020; 295:21.
30. Pan Y, Guan H, Zhou S, et al. Initial CT findings and temporal changes in patients with the novel coronavirus pneumonia (2019-nCoV): a study of 63 patients in Wuhan, China. *Eur Radiol* 2020; 30:3306-3309.
31. Xie X, Zhong Z, Zhao W, et al. Chest CT for typical coronavirus disease 2019 (COVID-19) pneumonia: relationship to negative RT-PCR testing. *Radiology* 2020; 296:E41-E45.
32. Chung M, Bernheim A, Mei X, et al. CT imaging features of 2019 novel coronavirus (2019-nCoV). *Radiology* 2020; 295:202-207.
33. Luchian ML, Lochy S, Motoc A, et al. Prognostic value of coronary artery calcium score in hospitalized COVID-19 patients. *Front Cardiovasc Med* 2021; 8:684528.
34. Xie X, Zhao Y, de Bock GH, et al. Validation and prognosis of coronary artery calcium scoring in nontriggered thoracic computed tomography: systematic review and meta-analysis. *Circ Cardiovasc Imaging* 2013; 6:514-521.
35. Giannini F, Toselli M, Palmisano A, et al. Coronary and total thoracic calcium scores predict mortality and provides pathophysiologic insights in COVID-19 patients. *J Cardiovasc Comput Tomogr* 2021; 15:421-430.
36. Rozanski A, Gransar H, Shaw LJ, et al. Impact of coronary artery calcium scanning on coronary risk factors and downstream testing the EISNER (Early Identification of Subclinical Atherosclerosis by Noninvasive Imaging Research) prospective randomized trial. *J Am Coll Cardiol* 2011; 57:1622-1632.
37. Gupta A, Lau E, Varshney R, et al. The identification of calcified coronary plaque is associated with initiation and continuation of pharmacological and lifestyle preventive therapies: a systematic review and meta-analysis. *JACC Cardiovasc Imaging* 2017; 10:833-842.